FULL LENGTH PAPER

ANALYSIS OF FUNCTIONALLY GRADED PLATES AND SHELLS: STRESS, BUCKLING AND FREE VIBRATION

Monslin Sugirtha Singh
Department of Civil Engineering
Sathyabama University, Jeppiaar Nagar
Chennai-600 119, India

Kari Thangaratnam
Department of Civil Engineering
DMI College of Engineering
Chennai-600 123, India
Email : drkari@yahoo.com

Abstract

Finite element formulation for Functionally Graded Material (FGM) thin shells subjected to Thermal and Mechanical loads are presented. The power law distribution model is assumed for the composition of the FGM material along the thickness. A software program "COMSAP" has been developed using Semiloof shell element formulation and validation checks are carried out using the results available in the related literature. Results for stress, buckling and vibration analysis of functionally graded shells are reported.

***Key words**: FGM, Thermal Stress, Shell, Buckling, Vibration*

Nomenclature

[A] = Extension stiffness matrix
[B] = Coupling stiffness matrix
[D] = Bending stiffness matrix
E = Young's modulus
$[f_m]$ = Consistent nodal load vector due to mechanical load
$[f_T]$ = Consistent nodal load vector due to thermal load
h = Thickness of shell
[H] = Strain matrix
[Q] = Reduced stiffness matrix of functionally graded material
$[K_s]$ = Structural stiffness matrix
$[K_G]$ = Geometric stiffness matrix
[M] = Mass matrix
M = Moment resultant
M^T = Thermal moment resultant
N = Force resultant
N^T = Thermal force resultant
p_o = Outer surface of shell made up of material 1
p_i = Inner surface of shell made up of material 2
q = Nodal displacement
R = Radius of shell
V1 = Volume of material 1
V2 = Volume of material 2
ΔT = Difference in temperature
α = Coefficient of linear thermal expansion
v = Poisson's ratio
λ = Eigen value
ω = Natural frequency

Introduction

Functionally Graded Materials (FGM) are heterogeneous composite materials usually made from a mixture of two different materials. The material properties of FGM are graded continuously and are controlled by the variation of the volume fraction of the constituent materials. FGM have the advantage of their ability to withstand high temperature gradients unlike fiber matrix composites, which show mismatch of mechanical properties across the interface of two discrete materials bonded together and resulting in de-bonding at high temperatures in some cases. FGM are now being strongly considered as a potential structural material for high-speed spacecraft, engine components which encounter extremely high cyclic thermal loads.FGM represent a rapidly developing area of Science and Engineering with numerous practical applications in nuclear projects, space projects and energy sector.

Paper Code : V66 N2/803-2014. Manuscript received on 17 Dec 2012. Reviewed, revised and accepted as a Full Length Contributed Paper on 24 Feb 2014

Literature Review

Over the past years, extensive research has been carried out on the modeling of FGM plates and shells [1-3]. The investigations were carried out in the existing literature for the stress, free vibration and buckling of FGM plates, concluding that 3D analytical solutions for FG plates are very useful than 2D plate theories. El-Abbasi and Meguid [4] presented a new thick shell element which accounts for thickness strain and stresses. Finite element formulation for thermoplastic analysis of FG Plate and shell were presented by Naghadabadi and Kordkheili [5], using eight noded degenerated shell element. Arciniega and Reddy [6] formulated shell element based on first order shear deformation theory with seven parameter and higher order lagarngian element. Pradyumna et. al [7] presented formulation for geometric nonlinear transient analysis based on higher order eight noded C° element with nine degrees of freedom per node. Formulation of cylindrical shell element based on classical shell theory is given by Setareh and Mlsvandzibael [8] for FGM cylindrical shells.

From the literature review, it is found that very few papers are available in this area of FEM for thin shells subjected to thermo mechanical loading. In order to get better accuracy of results for practical structures (thin plates and shells) Semiloof shell element is preferred for the analysis of structures, developed by Irons [9] thin structures and also Semiloof shell element which is successfully used for buckling, vibration, geometric non-linear analysis, non-linear vibration analysis for isotropic and composite thin plate and shell [10-12], is extended to FGM plates and shells.

Materials Modelling

FGM are microscopically inhomogeneous materials made from a mixture of two different materials, the composition continuously varies such that the upper surface (z=h/2) of the plate is material 1 whereas the lower surface (z=-h/2) is material 2 as shown in Fig.1. The effective material properties of Functionally Graded Materials P can be expressed as

$$P = p_o V1 + p_i V2 \tag{1}$$

p_o = Temperature dependent properties of outer surface of shell made up of material 1.

p_i = Temperature dependent properties of inner surface of shell made up of material 2.

V1 and V2 are volume fractions of material 1 and material 2 and related by

$$V1 + V2 = 1 \tag{2}$$

For a shell with a uniform thickness "h" and a reference surface at its middle surface, the volume fraction can be written as

$$Vc = \left(\frac{2z+h}{2h}\right)^n \tag{3}$$

z - Distance in thickness direction

Where n is the power law exponent,

$0 \le n \le \infty$

$$p(z) = (p_o - p_i)\left(\frac{2z+h}{2h}\right)^n + p_i \tag{4}$$

Where p_o and p_i are the corresponding properties of upper and lower surface.

The material properties along the thickness of the shell, such as Young's modulus E(z), Poisson's ratio ϑ(z) and the coefficient of thermal expansion α(z), can be determined according to Eq. (4). With these material properties, the stresses can be determined as

$$\{\sigma\} = \begin{Bmatrix}\sigma_x\\ \sigma_y\\ \tau_{xy}\end{Bmatrix} = \frac{E(z)}{1-\upsilon^2(z)}\begin{bmatrix}1 & \upsilon(z) & 0\\ \upsilon(z) & 1 & 0\\ 0 & 0 & \frac{1-\upsilon(z)}{2}\end{bmatrix}\left[\begin{Bmatrix}\varepsilon_x\\ \varepsilon_y\\ \gamma_{xy}\end{Bmatrix} - \begin{Bmatrix}\varepsilon_{xT}\\ \varepsilon_{yT}\\ \gamma_{xyT}\end{Bmatrix}\right]$$

$$= [Q]\left[\{\varepsilon\} - \{\alpha(z)\Delta T\}\right] \tag{5}$$

[Q] - Reduced stiffness matrix

Where E(z), ϑ(z), α(z) and ΔT are the Young's Modulus, Poisson's ratio, coefficient of linear expansion and temperature referenced to the stress free state respectively.

The axial force N and the moment M can be calculated using the following expression.

$$\left(N_{ij}\ M_{ij}\right) = \int_{-h/2}^{h/2} (1\ ,\ z)\ \sigma_{ij}\ dz \qquad (6)$$

Hence we have

$$\{N\} = [A]\ \{e\} + [B]\ \{k\} - \{N^T\}$$

$$\text{And } \{M\} = [B]\ \{e\} + [D]\ \{k\} - \{M^T\}$$

In which [A], [B], and [D] matrices are extension stiffness, coupling stiffness and bending stiffness respectively. Where

$\{e\}$ - strain vector

$\{k\}$ - curvature vector

$$([A], [B], [D]) = \int_{-h/2}^{h/2} (1, z, z^2)\ [Q]\ dz \qquad (7)$$

And the thermal force N^T and the thermal moment M^T are given by

$$\{N^T, M^T\} = \int_{-h/2}^{h/2} [Q]\ \{\alpha(z)\}\ \Delta T\ (1\ ,\ z)\ dz \qquad (8)$$

Finite Element Formulations

Semiloof shell element has all the advantages of Isoparametric formulation and uses Isoparametric shell theory and Discrete Kirchhoff Theory which can overcome the locking phenomenon. The quadrilateral semiloof shell element where the local coordinate system (X,Y,Z), Isoparametric curvilinear coordinates system (R,S,T) is illustrated in Fig.2. The semiloof element is first formulated with 43 degrees of freedom, (d.o.f).

- Four corner nodes and four mid side nodes possessing 3 degrees of freedom (d.o.f) u,v,w along the global x,y,z, direction respectively,
- Eight loof nodes, two on each side, located at the Gaussian quadrature position ($+1/\sqrt{3}$, $-1/\sqrt{3}$) and having two rotational d.o.f (θ_{xz} and θ_{yz}) along and perpendicular to the edge respectively,
- 3 d.o.f u,v,w at the central node.

Of those, 11 are eliminated by Kirchhoff shear constraint, so that the final version of the element has 32 d.o.f as follows.

- Four corner nodes and four mid side nodes possessing 3 d.o.f u,v,w.
- Eight loof nodes, having one rotational d.o.f θ_{xz}.

The geometry of the element is described by eight node Serendipity-type shape function. The displacement vector u [10] is given as

$$[u] = [d]\ [q] \qquad (9)$$

Where [q] - Nodal degree of freedom.
[d] - Shape function

Finite Element Formulation for Stress

The Finite Element Formulation is based on minimization of the total potential energy. The total potential energy Π of the functionally graded shell subjected to axial load may be written as

$$\Pi = \Sigma^m \int \frac{1}{2} \begin{bmatrix} e \\ k \end{bmatrix}^T \begin{bmatrix} A & B \\ B & D \end{bmatrix} \begin{bmatrix} e \\ k \end{bmatrix} da - \int [q]^T\ [d]^T\ [p]\ da$$

$$- \int \begin{bmatrix} e \\ k \end{bmatrix}^T \begin{bmatrix} N^T \\ M^T \end{bmatrix} da \qquad (10)$$

$$\begin{bmatrix} e \\ k \end{bmatrix} = [H]\ [q] \qquad (11)$$

Where [H] is the strain matrix [12, 13]. Substituting Eq. (11) in Eq. (10)

$$\Pi = \Sigma^m \int \frac{1}{2} [q]^T\ [H]^T\ [C]\ [H]\ [q]\ da - \int [q]^T\ [d]^T\ [p]\ da$$

$$- \int [q]^T\ [H]^T \begin{bmatrix} N^T \\ M^T \end{bmatrix} da \qquad (12)$$

$$\text{Where } [C] = \begin{bmatrix} A & B \\ B & D \end{bmatrix} \text{ and m - Number of elements} \qquad (12a)$$

Differentiating the total potential energy with respect to nodal displacement [q] and equating to zero gives

$$\Sigma^m \int [H]^T\ [C]\ [H]\ [q]\ da - \int [q]^T\ [p]\ da - \int [H]^T \begin{bmatrix} N^T \\ M^T \end{bmatrix} da = 0 \qquad (13)$$

[p] - Mechanical load vector

$$[K_S]\,[q] = [f_M] + [f_T] \tag{14}$$

$[f_M]$ - Consistent nodal force vector due to mechnical load.

$$[f_M] = \Sigma \int [d^T]\,[p]\; d\,a \tag{15}$$

$[f_T]$ - Consistent thermal load vector.

$$[f_T] = \int [H]^T \begin{bmatrix} N^T \\ M^T \end{bmatrix} d\,a \tag{16}$$

$[K_S]$ - Structural stiffness matrix.

$$[K_S] = \Sigma^m \int \left[[H]^T\,[C]\,[H] \right] da \tag{17}$$

Finite Element Formulation for Buckling

The work done due to the prebuckling stress during buckling is expressed as [10]

$$w = \frac{1}{2}\Big(N_{XX}\left[U_X^2 + V_X^2 + W_X^2\right] + N_{YY}\left[U_Y^2 + V_Y^2 + W_Y^2\right] + 2N_{XY}\left[U_X\,U_Y + V_X\,V_Y + W_X\,W_Y\right]\Big) \tag{18}$$

$$w = \frac{1}{2}\begin{Bmatrix} U_X \\ U_Y \\ V_X \\ V_Y \\ W_X \\ W_Y \end{Bmatrix} \begin{bmatrix} N_{XX} & N_{XY} & 0 & 0 & 0 & 0 \\ N_{XY} & N_{YY} & 0 & 0 & 0 & 0 \\ 0 & 0 & N_{XX} & N_{XY} & 0 & 0 \\ 0 & 0 & N_{XY} & N_{YY} & 0 & 0 \\ 0 & 0 & 0 & 0 & N_{XX} & N_{XY} \\ 0 & 0 & 0 & 0 & N_{XY} & N_{YY} \end{bmatrix} \begin{Bmatrix} U_X \\ U_Y \\ V_X \\ V_Y \\ W_X \\ W_Y \end{Bmatrix} \tag{19}$$

$$w = \frac{1}{2}[s]^T\,[P]\,[s] \tag{20}$$

$$[s]^T = [U_X, U_Y, V_X, V_Y, W_X, W_X] \tag{21}$$

$$[s] = [G]\,[q] \tag{22}$$

[G] - Shape function matrix of displacement and its derivative.

Substituting Eq. (22) in Eq. (20)

$$w = \frac{1}{2}[q]^T\,[G]^T\,[P]\,[G]\,[q] \tag{23}$$

The total potential energy for the buckling state can be written as

$$\pi_c = \sum^m \int \left[\frac{1}{2}[q]^T\,[H]^T\,[C]\,[H]\,[q] + \frac{1}{2}[q]^T\,[G]^T\,[P]\,[G]\,[q] \right] da \tag{24}$$

From the Eq.(24), Geometric Stiffness Matrix [13] can be written as

$$[K_G = \Sigma^m \int \left[[G]^T\,[P]\,[G] \right] da \tag{25}$$

In order to establish the critical buckling state corresponding to neutral equilibrium condition, the second variation of the total potential energy must be equal to zero.

$$\text{Hence } | [Ks] + \lambda\,[KG] | = 0 \tag{26}$$

Where λ is the Eigen value which multiplies the applied load to give the critical buckling loads.

Finite Element Formulation for Free Vibration

The governing equation can be derived from the Lagrangian Equations,

$$d/dt\,(\partial L/\partial \dot{q}i) - \partial L/\partial\, qi = 0\,, \quad i = 1\,,2\,,3 \tag{27}$$

Where L is the Lagrangian, defined as $L = T - \Pi$ (28)
and T is the kinetic energy

The kinetic energy for an element is defined as

$$T = \frac{1}{2}\rho h \int \left[\dot{u}^2 + \dot{v}^2\,\dot{w}^2 \right] da \tag{29}$$

$$T = \frac{1}{2}\int \{\dot{u}\}^T\,[p_m]\,\{\dot{u}\}\,da \tag{30}$$

$$\text{Where} \{\dot{u}\}^T = \{\dot{u}\,,\dot{v}\,,\dot{w}\} \tag{31}$$

$$[p_m] = \begin{bmatrix} ph & 0 & 0 \\ 0 & ph & 0 \\ 0 & 0 & ph \end{bmatrix} \tag{32}$$

The vector u can be defined as

$$\{\dot{u}\} = [d]\{\dot{q}\} \quad (33)$$

Substituting Eq.(330 in Eq.(30)

$$T = \frac{1}{2}\{\dot{q}\}^T [M]\{\dot{q}\} \quad (34)$$

Where mass matrix

$$[M] = \sum^{m} \int \left[[d]^T [p_m] [d] \right] da \quad (35)$$

Applying the langrangian equation Eq.(27) the governing equation for the free vibration can be written as

$$[Ks]\ [q] - [M]\ [\{\dot{q}\}] = [0] \quad (36)$$

Assuming harmonic oscillation the above equation can be written as

$$[Ks] - \omega^2\ [M]\ [q] = [0] \quad (37)$$

Where ω is natural frequency

Verification of the Program

The software package "COMSAP" developed by using semiloof shell element formulated by Kari Thangaratnam et al. [10-12] have the following capabilities.

- Mechanical and thermal stress analysis.
- Linear buckling analysis.
- Extended linear buckling analysis considers the pre-buckling deformation.
- Nonlinear analysis to find out snap through and bifurcation buckling.
- Free vibration.
- Large amplitude vibration.

In this work, FGM material model is added and verified with exact solutions and existing FEM results.

FGM Plates Under Uniform Pressure

Figure 3 shows central deflection versus the volume fraction exponent 'n' for FGM square plates under uniform pressure load [13]. The material properties Young's modulus and Poissons ratio for zirconia and aluminum are Ez=151GPa, v_z=0.3, Ea=70GPa, v_a=0.3 respectively. The quarter of the plate is modeled with 3x3 mesh and symmetric condition applied. Comparisons of the exact values with present results are very good.

Thermal Buckling of FGM Plate

FGM square plate composed of Alumina (Al_2O_3) and Nickel (Ni) is subjected to uniform temperature rise with clamped boundary condition [14]. The geometric parameters used are aspect ratio, a/h=100, span a=1m. Critical temperature for different volume fraction index obtained is compared in Table-1 and good agreement is observed between the two even for a coarse mesh 3x3.

Free Vibration of FGM Shell

Functionally graded cylindrical shell with length (L) =20m, radius(R) =1.0 m thickness (h) = .002m is considered from Ref. [15]. Both the edges are simply supported. Symmetric conditions prevail at the mid length and the cylinder buckles in 2 circumferential full waves (mc=2) and one axial wave (ma=1). Results of convergence study are given in Table-2 and compared well with results from Ref. [15].

Table-1 : Critical Temperature with Respect to Volume Fraction Index

Volume Fraction Index (n)	Critical Temperature Ref [14]	Critical Temperature Present Result
.3	28.21	27.47
1	30.56	29.78
5	34.17	35.93

Table-2 : Convergence Study of Vibration of Functionally Graded Cylindrical Shell (L/R=20., h/R=0.002, ma=1, mc=2)

Mesh (Axial x Circumferential)	Frequency (Hz) Present Value at ma=1	Frequency (Hz) at ma=1 Ref.{15}	% of Error
2 x 4	4.04	4.480	10.89
4 x 4	4.24	4.480	5.6
6 x 4	4.420	4.480	1.3

Results and Discussion

For the analysis of shell material 1, 2 and 3 as in Table-3 are used. The material properties are calculated at room temperature (T=27°C) [16-18].

Shells Subjected to Uniform Pressure

A quadrant of the shell is considered based on the symmetric conditions and modeled using 6x4 mesh. The geometric parameters used are Length, L=1m, Radius R=1m, Thickness h=.01m, angle θ=90° . The shell is subjected to uniform pressure of 0.1kPa and the displacement at centre of the shell is reported for different boundary conditions such as clamped immoveable, clamped movable and simply supported movable in Fig.4, Fig.5 and Fig.6 respectively.

It is observed that as the volume fraction increases, the displacement also increases for the different boundary conditions as the property changes from ceramic to metal. The displacement varies as volume fraction increases from 0 to 2 and then the variation is less and it is due to the variation of extensional and bending stiffness of the material.

Shell Subjected to Temperature Load

A quadrant of the shell is considered for the symmetric conditions and modeled using 6x4 mesh.The length of the shell is L=1m, Radius R=1m, Thickness h=.01m. The shell is subjected to linear temperature variation (0 to 100°C) through thickness and the displacements are studied for the two boundary conditions clamped moveable and clamped immovable and given in Fig.7 and Fig.8. In the case of thermally stressed shells, for materials 1, 2 and 3, the displacement increases as the volume fraction increases and then decreases when n is equal to 5, whereas for material 2 the displacement starts decreasing when n is equal to 2. The variation of the moment resultant along the length of shell is given for clamped movable shell in Fig.9 and in Fig.10 for material 1 and 2 respectively for different volume fraction index from n=0 to 5.The moment resultants increases locally, along the length up to 0.25y/L and thereafter decreases up to 0.1y/L and then increases and remains constant after 0.3y/L for material 1 and 2 for all volume fractions. For material 1 the moment resultants decreases as volume fraction index increases from 0 to 2 and increases after n is 5 but for material 2 the moment resultants decreases as volume fraction index increases from 0 to 0.4 and increases after n is 0.8.

Buckling of Shells Under Axial Load

A quadrant of the shell is analyzed considering the symmetric conditions and modeled using 6x4 meshes. The Radius(R) of the shell 1cm, thickness (h) is 0.03 cm and material 4 is used in this analysis. For various L/R ratios buckling loads are calculated for simply supported (SS) and clamped clamped (CC) boundary conditions and the results are shown in Fig.11 and Fig.12. From the graphs it is seen that the well known result buckling load decreases rapidly as L/R ratio increases, since the slenderness ratio increases as length increases. In all above cases circumferential wave (mc) is 2 and axial wave (ma) varies from 13, 13, 11, 11, 9 and 9 for different L/R ratio 5, 10, 20, 30, 40 and 50 respectively for clamped clamped shells. For simply supported shells circumferential wave (mc) is 2 and axial wave (ma) varies 12, 11, 11, 8, 8 and 7 for different L/R ratio 5, 10, 20, 30, 40 and 50 respectively.

Table-3 : Material Properties of the FGM Materials

FGM Material Number	FGM Material	E gpa	**v**	ρ (kg/m^3)	α ° C
Material 1 Ref [16]	Aluminum (Al)	70.	0.3	2707	23 x 10^{-6}
	Zirconia (ZrO2)	151	0.3	3000	10 x 10^{-6}
Material 2 Ref [16]	Ti-6Al-4v	105.6	0.3	4420	6.94 x 10^{-6}
	Alumina (Al203)	320.2	0.3	3970	7.2 x 10^{-6}
Material 3 Ref [17]	Titanium (Ti)	105.8	0.3	4420	8.4 x 10^{-6}
	Silicon Carbide (SiC)	410	0.17	3100	4.3 x 10^{-6}
Material 4 Ref [18]	Stainless Steel	207.78	0.31	8166	10.1 x 10^{-6}
	Zirconia	168.04	0.2885	5700	10 x 10^{-6}

Free Vibration of Cylindrical Shell

Natural frequency of a functionally graded shell having R=1 m, h=002 is considered. Material 4 is used for analysis. Natural frequencies of a functionally graded shell for various L/R ratios (5, 10, 20, 30, 40 and 50) for both the simply supported and clamped - clamped boundary conditions given in Fig.13 and Fig.14. In both the boundary conditions natural frequency decreases rapidly as L/R ratio increases. It is also noted that the natural frequency decreases gradually as the material changes from zirconia to stainless steel, since the Young's modulus of zirconia is greater than stainless steel and the Young's modulus of FGM is based on the volume fraction of the two materials and lies in between them. For both boundary conditions circumferential wave (mc) is 2 and axial wave (ma) is 1 for different L/R ratio.

Conclusion

The Finite element formulation using semiloof shell element for functionally graded material modeling is presented. The accuracy of the numerical results is verified with the existing results from the reviewed literature and the results are agreeing well. The displacement under uniform pressure load and thermal load are studied for cylindrical shell. For the thermal load the displacement behavior is different from mechanical load behavior and it is influenced by the thermal force and moment resultants, which is mainly due to the coefficient of thermal expansion variation in constituent materials. For shells the L/R ratio increases the buckling load and frequency decreases. From the results it is clear that constituent volume fractions and configuration of the constituent materials affect the natural frequency and buckling Load.

References

1. Birman, V. and Byrd, W.L., " Modeling and Analysis of Functionally Graded Materials and Structures", Appl. Mech. Rev, Vol .60, Sep. 2007, pp.195-216.

2. Ebrahimi, F., Sepiani, H.A. and Arani, A.G., "Progress in Analysis of Functionally Graded Structures", Nova Science Publishers Inc., New York, 2011.

3. Jha, D.K., Tarun Kant and Singh, R.K., "A Critical Review of Recent Research on Functionally Graded Plates", Compo. Struct., Vol.96, 2013, pp.833-849.

4. Abbasi, N.EL. and Meguid, S.S., "Finite Element Modeling of the Thermo Elastic Behavior of Functionally Graded Plates and Shells", Int. J of Comput. Engg. Sci., Vol.1, 2000, pp.151-165.

5. Naghadabadi, R. and Kordkheili, S.A.H., "A Finite Element Formulation for Analysis of Functionally Graded Plates and Shells", Archive of Applied Mechanics, Vol.74, 2005, pp.375-386.

6. Arciniega, R.A. and Reddy, J.N., "Large Deformation Analysis of Functionally Graded Shells", Int. J. of Solid and Struct., Vol.44, 2007, pp.2036-2052.

7. Pradyumna, S., Namita Nanda and Bandyopadhyay, J.N., "Geometrically Nonlinear Transient Analysis of Functionally Graded Shell Panels Using Higher-order Finite Element Formulation", J. of Mech. Engg. Res., Vol.2(2), 2010, pp.39-51.

8. Setareh, M. and Isvandzibael, M.R., "Comparison of Two Types Material for Vibration FGM Cylindrical Shell", J. Basic Appl. Sci. Res., Vol.1, 2011, pp.1228-1235.

9. Irons, B.M., "The Semiloof Shell Element", Proceedings of the Conference on Finite Elements for Thin Shell and Curved Members, London, 1974, pp.197-222,

10. Thangaratnam. R.K., Palaninathan and Ramachandran J., "Thermal Stress Analysis of Laminated Composite Plate and Shells", Comput. Struct., Vol.30, No.6, 1988, pp.1403-1411.

11. Thangaratnam. R.K., Palaninathan and Ramachandran J., "Thermal Buckling of Composite Laminated Plates", Comput. Struct., Vol.32, No.5, 1989, pp.1117-1124.

12. Thangaratnam. R.K., Palaninathan and Ramachandran J., "Thermal Buckling of Laminated Composite Shells", AIAA J., Vol.28, May 1990, pp.859-860.

13. Aleman RAA., "On a Tensor- Based Finite Element Model for the Analysis of Shell Structures", Ph.D. Thesis, Texas A and M University, 2005.

14. Kyung-su and ji-Hwan Kim, "Three Dimensional Thermal Buckling Analysis of Functionally Graded Material", Compos. Part B, Vol.35, 2004, pp.429-437.

15. Loy, C.T. and Reddy, J.N., "Vibration of Functionally Graded Cylindrical Shells", Int. J . Mech. Sci., Vol.41, Mar 1999, pp.309-324.

16. Zhao, X. and Liew, K.M., "A Mesh Free Method for Analysis of the Thermal and Mechanical Buckling of FG Cylindrical Panels", Computational Mech., Vol.45, 2010, pp.297-310.

17. Vel, S.S., "Exact Elasticity Solution for the Vibration of Functionally Graded Anisotropic Cylindrical Shells", Compos. Struct., Vol.92, 2010, pp.2712-2727.

18. Yang J., "Nonlinear Analysis of Functionally Graded Plates Under Transverse and Inplane Loads", Int. J. Non Linear Mech., Vol.38, June 2003, pp. 467-482.

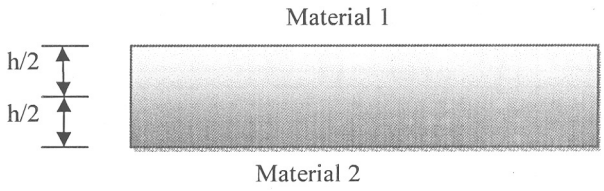

Fig.1 Functionally Graded Plate

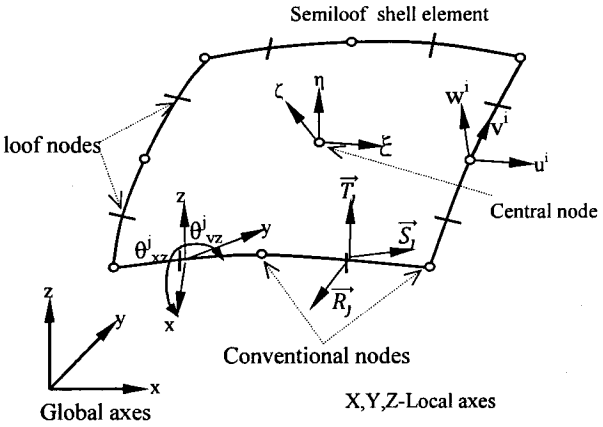

Fig.2 Semiloof Shell Element

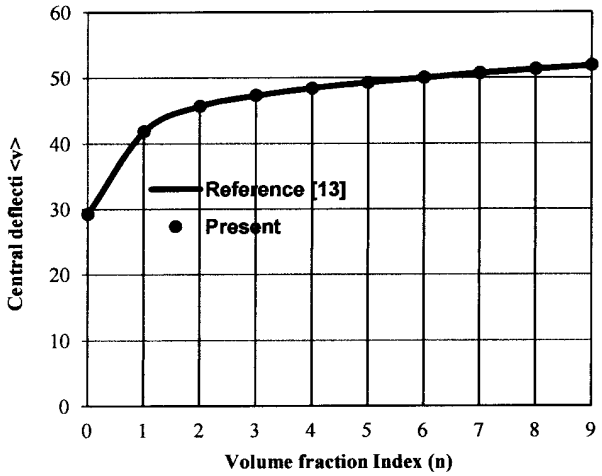

Fig.3 Central Deflection of a Square Plate Under Uniform Load

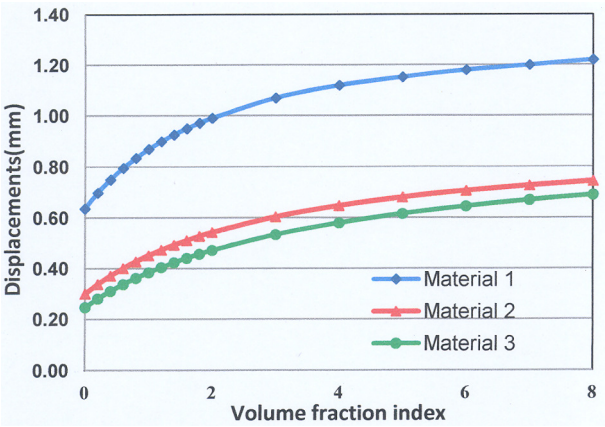

Fig.4 Displacement at Centre of Clamped Immoveable Shell Under Uniform Pressure

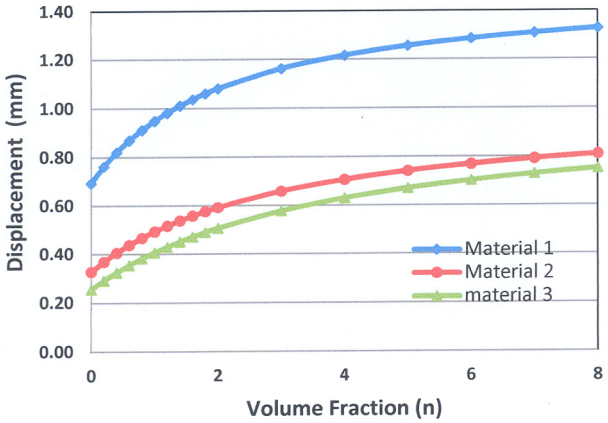

Fig.5 Displacement at Centre of Clamped Moveable Shell Under Uniform Pressure

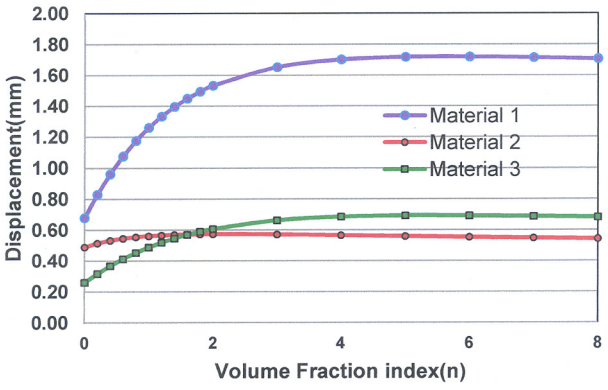

Fig.8 Displacement at Centre of Clamped Immoveable Shell Under Thermal Load

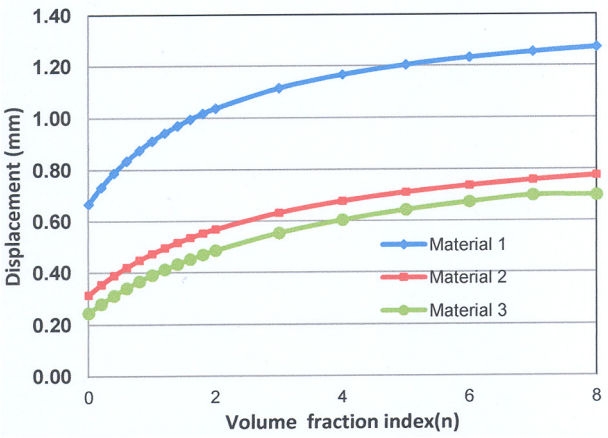

Fig.6 Displacement at Centre of Simply Supported Moveable Shell Under Uniform Pressure

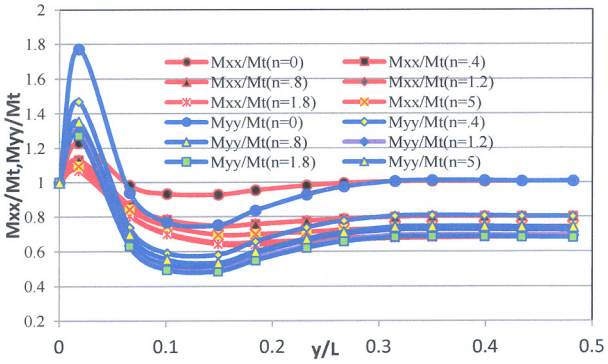

Fig.9 Moment Resultant Along the Length of Cylindrical Shell for Material1

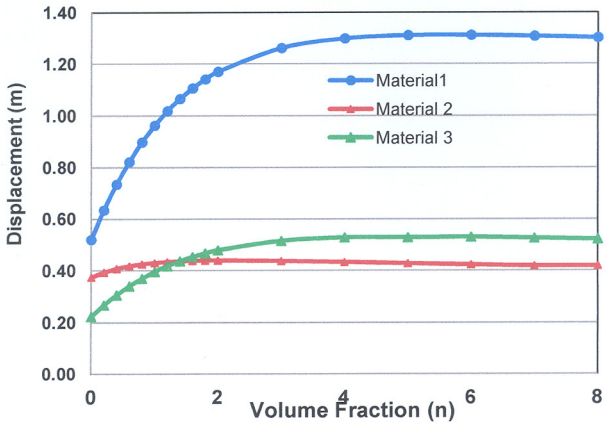

Fig.7 Displacement at Centre of Clamped Moveable Shell Under Thermal Load

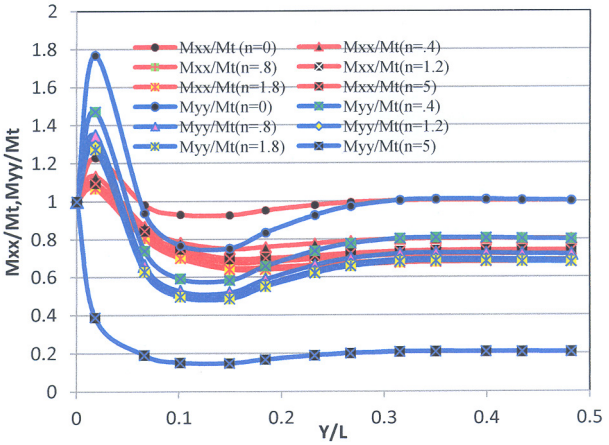

Fig.10 Moment Resultant Along the Length of Cylindrical Shell for Material2

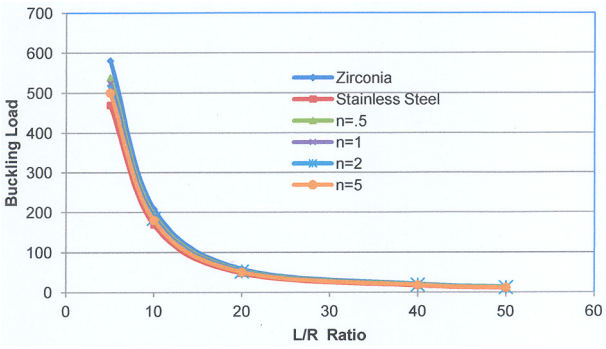

Fig.11 Buckling Load Against L/R Ratio (ma=1, h/R=20) for Simply Supported Boundary Conditions

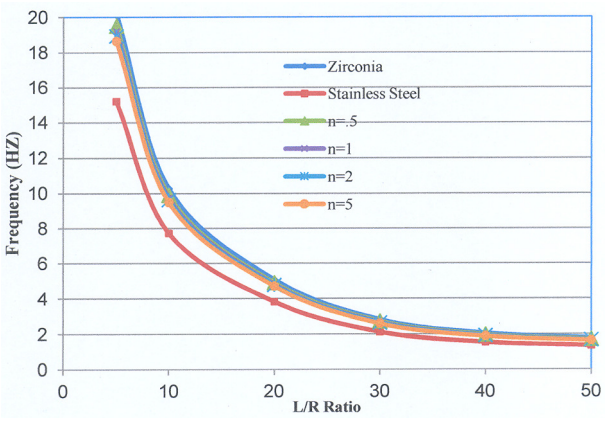

Fig.13 Natural Frequency Against L/R Ratio for Simply Supported Boundary Condition

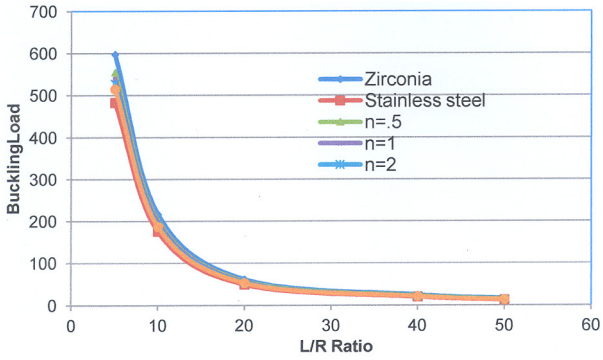

Fig.12 Buckling Load Against L/R Ratio (ma=1, h/R=20) for Clamped Clamped Boundary Conditions

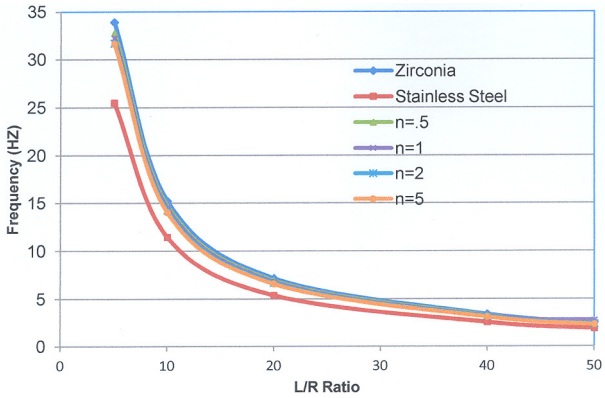

Fig.14 Natural Frequency Against L/R Ratio for Clamped Clamped Boundary